AD-A048 695 AEROSPACE CORP EL SEGUNDO CALIF IVAN A GETTING LABS F/G 16/3
LINEARIZED NEWTONIAN AERODYNAMICS OF SLENDER INFLATED CONES.(U)
DEC 77 J W ELLINWOOD F04701-77-C-0078
UNCLASSIFIED TR-0078(3940-02)-1 SAMSO-TR-77-218 NL

1 OF 1
AD
A048695

END
DATE
FILMED
2-78
DDC

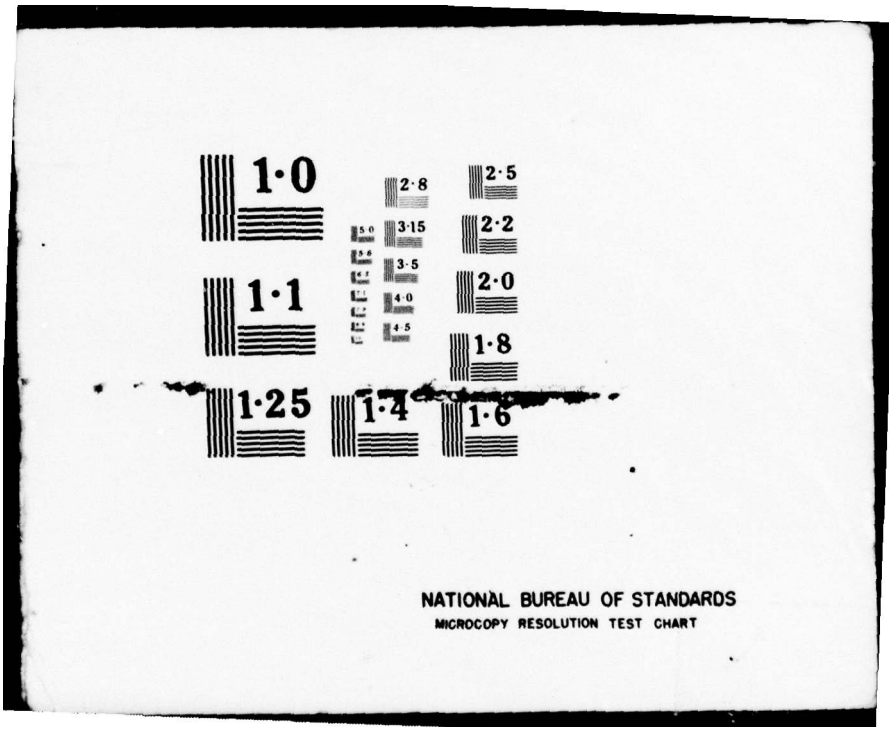
1·0
1·1
1·25
2·8
3·15
3·5
4·0
4·5
5·0
1·4
2·5
2·2
2·0
1·8
1·6
NATIONAL BUREAU OF STANDARDS
MICROCOPY RESOLUTION TEST CHART

REPORT SAMSO-TR-77-218

Linearized Newtonian Aerodynamics of Slender Inflated Cones

J. W. ELLINWOOD
Aerophysics Laboratory
The Ivan A. Getting Laboratories
The Aerospace Corporation
El Segundo, Calif. 90245

5 December 1977

Interim Report

Prepared for

SPACE AND MISSILE SYSTEMS ORGANIZATION
AIR FORCE SYSTEMS COMMAND
Los Angeles Air Force Station
P.O. Box 92960, Worldway Postal Center
Los Angeles, Calif. 90009

This interim report was submitted by The Aerospace Corporation, El Segundo, CA 90245, under Contract No. F04701-77-C-0078 with the Space and Missile Systems Organization, Deputy for Advanced Space Programs, P.O. Box 92960, Worldway Postal Center, Los Angeles, CA 90009. It was reviewed and approved for The Aerospace Corporation by W. R. Warren, Jr., Director, Aerophysics Laboratory. Lieutenant Dara Batki, SAMSO/YCPT, was the project officer for Advanced Space Programs.

This report has been reviewed by the Information Office (OI) and is releasable to the National Technical Information Service (NTIS). At NTIS, it will be available to the general public, including foreign nations.

This technical report has been reviewed and is approved for publication. Publication of this report does not constitute Air Force approval of the report's findings or conclusions. It is published only for the exchange and stimulation of ideas.

Dara Batki

Dara Batki, Lt, USAF
Project Officer

Robert W. Lindemuth

Robert W. Lindemuth, Lt Col, USAF
Chief, Technology Plans Division

FOR THE COMMANDER

Leonard E. Baltzell

Leonard E. Baltzell
Asst Deputy for Advanced Space Programs

UNCLASSIFIED

SECURITY CLASSIFICATION OF THIS PAGE (When Data Entered)

(19) REPORT DOCUMENTATION PAGE		READ INSTRUCTIONS BEFORE COMPLETING FORM
(18) 1. REPORT NUMBER: SAMSO-TR-77-218	2. GOVT ACCESSION NO.	3. RECIPIENT'S CATALOG NUMBER: (1)
(6) 4. TITLE (and Subtitle): LINEARIZED NEWTONIAN AERODYNAMICS OF SLENDER CONES. Inflated		5. TYPE OF REPORT & PERIOD COVERED: Interim rept.
		(14) 6. PERFORMING ORG. REPORT NUMBER: TR-0078(3940-02)-1
(10) 7. AUTHOR(s): John W. Ellinwood		(15) 8. CONTRACT OR GRANT NUMBER(s): F04701-77-C-0078
9. PERFORMING ORGANIZATION NAME AND ADDRESS: The Aerospace Corporation, El Segundo, Calif. 90245		10. PROGRAM ELEMENT, PROJECT, TASK AREA & WORK UNIT NUMBERS: (12) 37 p.
(11) 11. CONTROLLING OFFICE NAME AND ADDRESS: Space and Missile Systems Organization, Air Force Systems Command, Los Angeles, Calif. 90009		12. REPORT DATE: 5 December 1977
		13. NUMBER OF PAGES: 35
14. MONITORING AGENCY NAME & ADDRESS (if different from Controlling Office)		15. SECURITY CLASS. (of this report): Unclassified
		15a. DECLASSIFICATION/DOWNGRADING SCHEDULE

16. DISTRIBUTION STATEMENT (of this Report)

Approved for public release; distribution unlimited.

17. DISTRIBUTION STATEMENT (of the abstract entered in Block 20, if different from Report)

18. SUPPLEMENTARY NOTES

19. KEY WORDS (Continue on reverse side if necessary and identify by block number)

Inflated Bodies
Hypersonic Aerodynamics

20. ABSTRACT (Continue on reverse side if necessary and identify by block number)

Biconic vehicles covered with unsupported cloth are predicted to experience skin displacement from aerodynamic pressure at small angle of attack. The resulting shape, aerodynamic force, and moment perturbations are predicted as functions of given axial tension and internal pressurization. A tension parameter is identified that varies inversely as dynamic pressure. It is concluded that the inflatable loses its shape dramatically unless this tension parameter is at least of order one, and that this useful boundary cannot be appreciably extended by increasing pressurization, unless the internal

→ next page

DD FORM (FACSIMILE) 1473

409 944

UNCLASSIFIED

SECURITY CLASSIFICATION OF THIS PAGE (When Data Entered)

19. KEY WORDS *(Continued)*

20. ABSTRACT *(Continued)*

pressure is at least an order of magnitude larger than external pressures.

CONTENTS

FIGURES

INTRODUCTION

Inflated vehicles of biconic shape have been proposed for use as strategic ballistic weapons. The forecone and base disk would be relatively rigid and separated by an axial compression column (Fig. 1). The aft frustum would consist of fabric stretched between forecone and base and supported by internal pressurization. A major concern is that rising external pressures during reentry will increasingly displace the cloth surface and alter the aerodynamic characteristics of the "softened" vehicle until an altitude is reached below which the mission is compromised. The present theory predicts static aerodynamic derivatives for the perturbed ("banana") biconic.

Inflatable structures have been studied for many years. Just since 1972, articles have appeared on the shape of balloons, flexible deceleration devices, air bags for ground effect vehicles, inflated paragliders, inflated sails, inflated marine cantilevers, air springs, lighter-than-air vehicles, inflated pontoons, space inflatables, inflatable rocket nozzle extensions, etc. None of these is referenced here, because none describes an inflated yawed cone (nor, in fact, any inflated yawed shape in hypersonic flow).

The displacements expected (Fig. 1) depend generally on the imposed axial tension, the amount of internal pressurization, the elasticity of the frustum fabric, and the scale or size of surface deflection. The value of the present analysis is that it explicitly retains and displays the effects of two of these important features: the amount of axial tension and the amount of internal pressurization. Other features are necessarily omitted; we assume

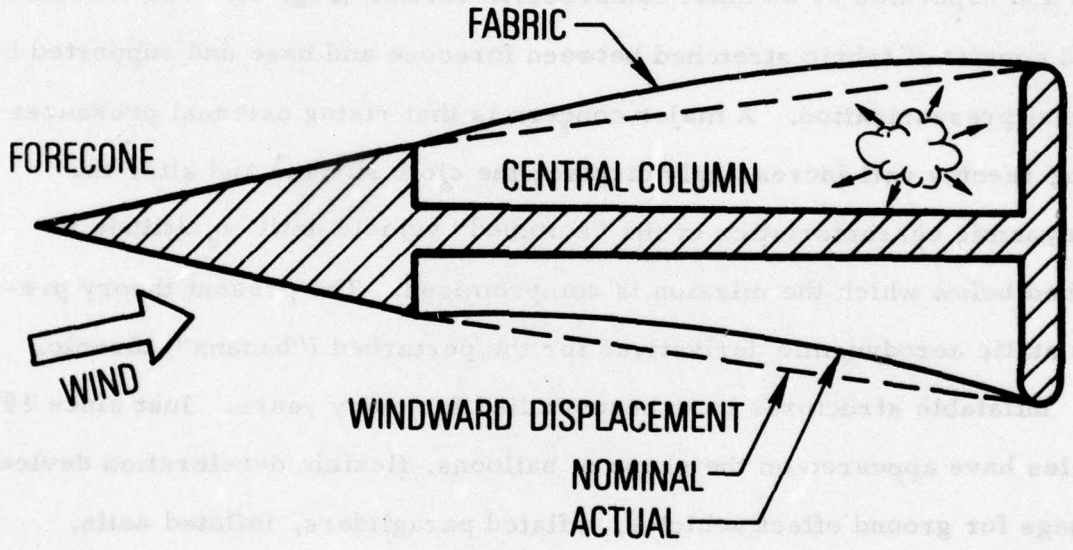

Fig. 1. Hypersonic Biconic Inflatable

that the cloth is inelastic (unless the level of pressurization is uniquely that which makes the unyawed, symmetric shape conical) and that the fabric displacement is small enough for the present linearized description. Three other assumptions are made that may be important in special applications: that the external pressures are Newtonian, the vehicle is slender and nonporous, and the angle of attack is small compared with the cone half-angle.

ANALYSIS

An axisymmetric biconic, whose rigid forecone has semiapex angle θ ($\theta \ll 1$) and length $\tau x_1/\theta$ (Fig. 2), and whose frustum has semiapex angle τ ($\tau \ll 1$) and theoretical length L, is placed in a hypersonic flow at small yaw angle α ($\alpha \ll \tau$). The bow shock wave is assumed to lie so close to the body ($M^2\tau^2 \gg 1$ and $\gamma - 1 \ll 1$, where γ is specific heat ratio) that external pressures can be approximated by Newtonian values.

PRESSURES ON AFT FRUSTUM

Let r be the radius in any cross section and ϕ the meridian angle measured from the windward ray, and let $\mu = \tan^{-1}(r_\phi/r)$, where subscript ϕ or x denotes differentiation of local radius r with respect to ϕ or x, respectively. Variables ϕ and μ are shown in Fig. 3a, which depicts what would be seen by an observer stationed at $x = 0$ and looking aft. Figure 3a is a spherical triangle whose legs are small angles. Because of the slender-body approximation, the laws of plane trigonometry apply in Fig. 3a. Without deformation, $r_x = \tau$ and $\mu = 0$. From the sine law

$$\beta = r_x \sin\mu/\sin\phi \ll 1;$$

$$\zeta = r_x \sin\phi/\sin(\phi - \mu) \ll 1$$

The Newtonian pressure coefficient is $2\cos^2\delta$, where δ is the angle between the downwind direction and the external surface normal. This nearly right angle is shown as one side of the spherical triangle in Fig. 3b. The angle $\phi - \mu$ is common to both Fig. 3a and Fig. 3b. From the cosine law for

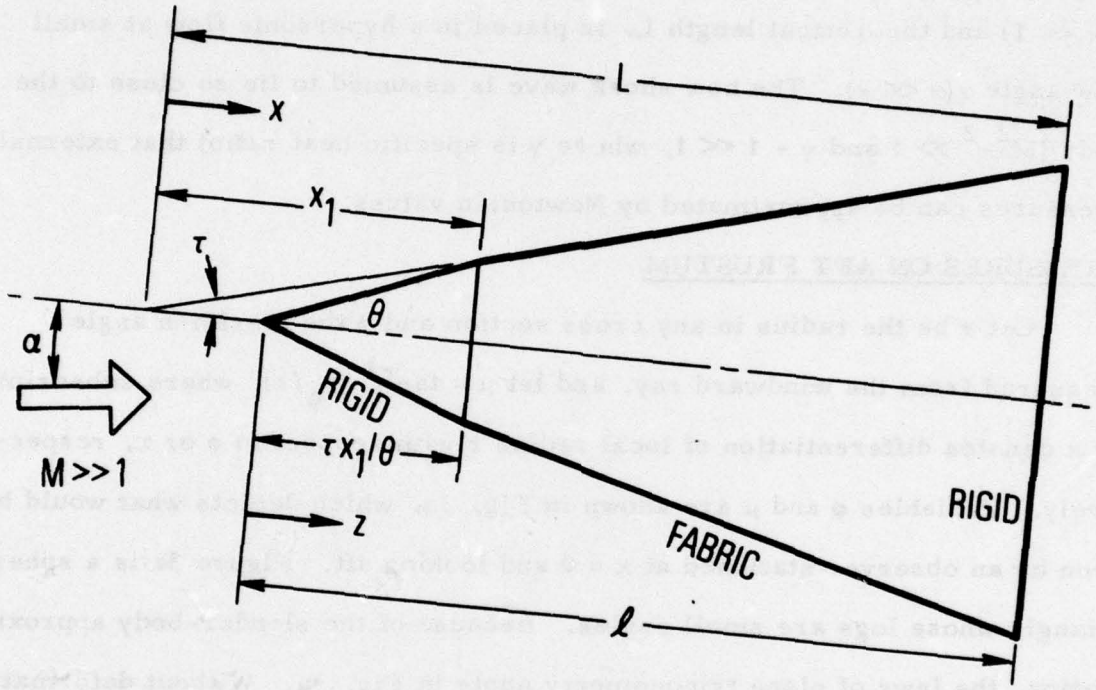

Fig. 2. Nomenclature

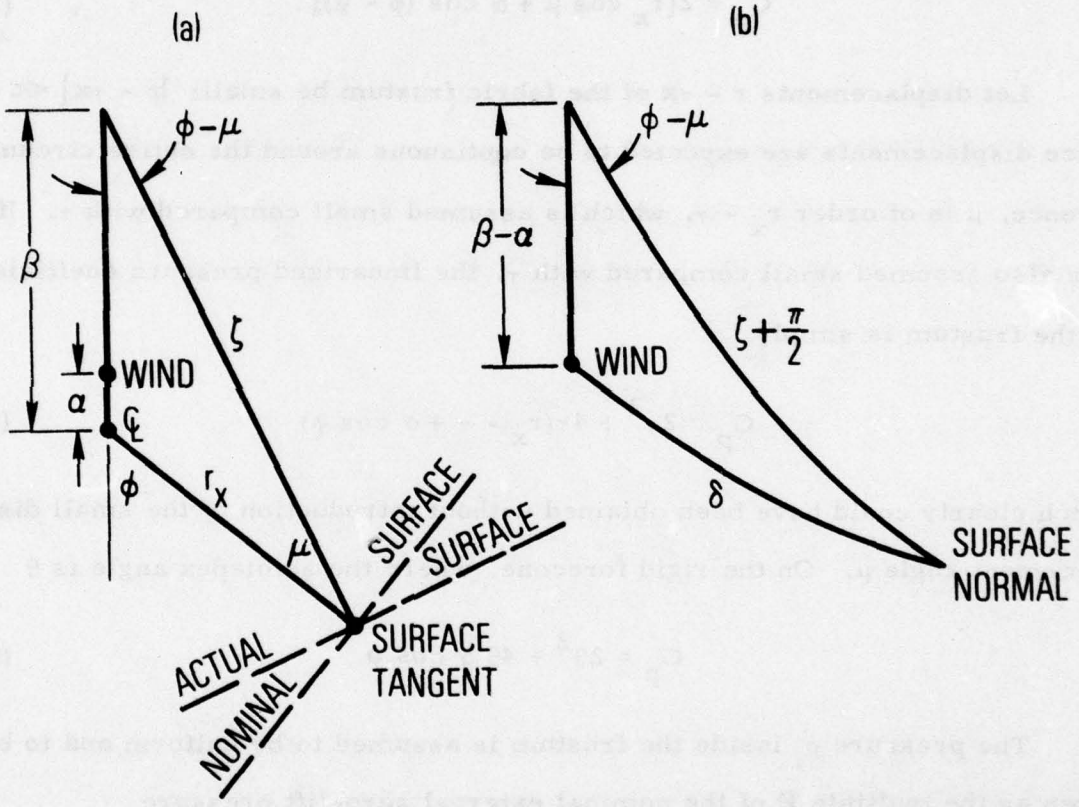

Fig. 3. Frustum Trigonometry

sides of a spherical triangle

$$\cos \delta = - \gamma + (\beta - \alpha) \cos (\phi - \mu)$$

Combination of these relations leads to the external pressure coefficient

$$C_p = 2[r_x \cos \mu + \alpha \cos (\phi - \mu)]^2 \qquad (1)$$

Let displacements $r - \tau x$ of the fabric frustum be small: $|r - \tau x| \ll \tau x$. Since displacements are expected to be continuous around the entire circumference, μ is of order $r_x - \tau$, which is assumed small compared with τ. If α is also assumed small compared with τ, the linearized pressure coefficient on the frustum is simply

$$C_p = 2\tau^2 + 4\tau(r_x - \tau + \alpha \cos \phi) \qquad (2)$$

which clearly could have been obtained without introduction of the small displacement angle μ. On the rigid forecone, where the semiapex angle is θ

$$C_p = 2\theta^2 + 4\theta \alpha \cos \phi \qquad (3)$$

The pressure p_i inside the frustum is assumed to be uniform and to be given as the multiple P of the nominal external zero-lift pressure

$$p_i/q = P2\tau^2$$

where q is dynamic pressure. The pressure difference $p_i - p_e$ ($\equiv \Delta p$) across the fabric is then

$$\Delta p/q = 2\tau^2(P - 1) - 4\tau(r_x - \tau + \alpha \cos \phi) \qquad (4)$$

FORCE COMPONENT EQUATIONS

Let the product of stress and skin thickness be denoted by T^x, T^ϕ, and $T^{x\phi}$. The first two are tensions per unit surface length in the axial and azimuthal directions, respectively. $T^{x\phi}$ is the shear force per length. In order for forces on a surface element of length dx and width $rd\phi$ to be in equilibrium, each component of force must vanish. For a slender body ($r_x \ll 1$) and small surface displacement ($r_\phi / r \ll 1$), the radial, axial, and azimuthal components are related, respectively, as

$$r\Delta p + (T^x r r_x)_x + (T^{x\phi} r_\phi)_x + (T^\phi r_\phi / r)_\phi + (T^{x\phi} r_x)_\phi - T^\phi = 0 \tag{5}$$

$$-\Delta p\, r r_x + (r T^x)_x + T^{x\phi}_\phi = 0 \tag{6}$$

$$-\Delta p\, r_\phi + T^\phi_\phi + (r\, T^{x\phi})_x = 0 \tag{7}$$

AXIAL TENSION

Our interest lies in small displacements from a conical shape ($r = \tau x$), such as the cone expected at zero angle of attack if the level of internal pressurization is that for which the cloth was shaped. The zero-order integrated form of Eq. (6), the axial component balance, is then

$$\tau x T^x = C + (1/2)\Delta p (\tau x)^2 \tag{8}$$

Physically, the constant C represents the compressive force ($\div 2\pi$) in the central column (Fig. 1) that stretches the fabric in the absence of aerodynamic pressures. When the zero-order form of Δp, given by Eq. (4), is used in the

second right-member term above (and it is naturally assumed that P is of order unity and x is of order L), this last term of Eq. (8) is found to be of order $q_\tau{}^4 L^2$. The present theory is intended to apply where the left member of Eq. (8) is, instead, of the lower order $q_\tau{}^2 L^2$. This intent is fulfilled when the zero-order axial tension is normalized as

$$xT^x = T2q_\tau L^2 \qquad , \qquad \tau^2 \ll T = \mathcal{O}(1) \tag{9}$$

Changes in Δp affect T^x only through the last term of Eq. (8), which is of order τ^2 compared with the constant term and is neglected in Eq. (9). Changes in skin length, which might affect T^x through axial elasticity, vary as the square of skin displacement and are similarly neglected. The normalized axial tension parameter T is thus a known parameter in the present linear treatment.

SHEAR STRESS

The circumferential or "hoop" tension per station, T^ϕ, is expected to consist of both zero- and first-order contributions. A physical reason for changes in T^ϕ being of first order when those in T^x are of second order is that the fabric skin is not fixed to a rigid frame on any meridian as it is at fore and aft stations. The shear force per length, $T^{x\phi}$, on the other hand, is of first order. There is no zero-order component of $T^{x\phi}$, because it is assumed that erection of this inflated vehicle was achieved without any torsion built in between the rigid forecone and base (Fig. 1).

Examination of the several terms in the left member of Eq. (5) reveals that the third and fifth terms involve $T^{x\phi}$. In the third term, both $T^{x\phi}$ and r_ϕ

are of first order; this term is therefore of second order and is neglected. The fifth term, $(T^{x\phi} r_x)_\phi$, contains only one possibly first-order term, namely, $T^{x\phi}_{\phi} r_\tau$. We can express this term as a function of displacement immediately by multiplying Eq. (6) by τ. However, these replacement terms for $T^{x\phi}_{\phi} r_\tau$ are of order $\Delta p\, r\tau^2$, which is small compared with $r\Delta p$, the first term of Eq. (5). As a result, both terms involving $T^{x\phi}$ can be omitted from Eq. (5).

Examination of the three terms in the left member of Eq. (7) reveals that the first term, $-\Delta p\, r_\phi$, must be considered as first order if $r\Delta p$ is called zero order. The third term, however, is of order $\tau T^{x\phi}$, which is of order $\tau T^{x\phi}_{\phi}$, a term that was found above to be of order $r\Delta p \tau^2$, i.e., of second order and negligible. On this basis, Eqs. (5) and (7) can and will be solved for small displacements of the skin on a slender cone without consideration of shear stress. Equation (5) with (9) then becomes

$$2\tau q\left[r\frac{\Delta p}{2\tau q} + TL^2\left(\frac{r r_x}{x}\right)_x\right] + T^\phi\left(\frac{r_{\phi\phi}}{\tau x} - 1\right) = 0 \qquad (10)$$

Equation (7) with (4) can be integrated to the form

$$T^\phi = T^\phi(0, x) + 2\tau^2 q(P - 1)[r - r(0, x)] \qquad (11)$$

HOOP STRESS

The windward circumferential tension per station, $T^\phi(0, x)$, consists of both zero- and first-order contributions when $P > 1$. The zero-order part, from Eq. (5), is the zero-order value of $r\Delta p$, namely $2\tau^3(P - 1)qx$. The first-order part will be called $\Delta T^\phi(0, x)$. Elimination of $T^\phi(\phi, x)$ between

Eqs. (10) and (11) and elimination of Δp by use of Eq. (4) lead to an equation for displacement r. When zero-order terms are removed, one is left with

$$\tau(P - 1)[r(0,x) - \tau x + r_{\phi\phi}] - 2\tau x(r_x - \tau + \alpha \cos \phi) + TL^2(rr_x/x)_x$$

$$- \Delta T^{\phi}(0,x)/2\tau q = 0, \qquad P > 1 \tag{12}$$

Because Eq. (12) describes the displacement on any meridian ϕ, the unknown function $\Delta T^{\phi}(0,x)$ can be replaced by the value on the windward meridian of all the other left-member terms in Eq. (12).

$$\tau(P - 1)r_{\phi\phi} - 2\tau x(r_x - \tau + \alpha \cos \phi) + TL^2(rr_x/x)_x$$

$$= \tau(P - 1)r_{\phi\phi}(0,x) - 2\tau x[r_x(0,x) - \tau + \alpha] \tag{13}$$

$$+ TL^2[r(0,x)r_x(0,x)/x]_x, \qquad P > 1$$

Care must be taken, however, to ensure that the hoop stress is non-negative, because compressive stresses cause membrane buckling immediately. T^{ϕ} is expected to vanish on all meridians when the vehicle is underpressurized ($P < 1$). In this situation, the circumference is expected to be reduced, with the surplus fabric being taken up in folds. These can be interior or exterior folds; the present analysis does not describe the folds. In this linear analysis, such reduction in circumference must be small and is treated as a first-order perturbation from the conical shape associated with $P = 1$, even at zero angle of attack. Specifically, when $0 < 1 - P \ll 1$, Eq. (12) becomes

$$\tau^2 x(P - 1) - 2\tau x(r_x - \tau + \alpha \cos \phi) + TL^2(rr_x/x)_x = 0 \tag{13}$$

There is a very narrow zone of internal pressures, intermediate between the external windward pressure and the slightly lower external leeward pressure, for which a positive hoop stress may occur over a limited range of (leeward) meridians. This transition range where $P \approx 1$ is not considered in detail, inasmuch as terms that were otherwise of first order are there no longer large compared with neglected second-order terms, such as those involving shear.

DISPLACEMENT WHEN $P > 1$

It is convenient to introduce dimensionless variables R and y for displacement and station as follows:

$$r - \tau x = R(\phi, y)\tau T^{1/2} L \quad ; \quad x = yT^{1/2} L \tag{14}$$

With this choice, T disappears from the differential equation:

$$(P - 1)R_{\phi\phi} - 2y\left(R_y + \frac{\alpha}{\tau}\cos\phi\right) + \left(\frac{R}{y} + R_y\right)_y$$

$$= (P - 1)R_{\phi\phi}(0, y) - 2y\left[R_y(0, y) + \frac{\alpha}{\tau}\right] + \left[\frac{R(0, y)}{y} + R_y(0, y)\right]_y \tag{15}$$

For boundary conditions, it is required that the displacement R vanish at the biconic shoulder (the forward end of the membrane) and at the base, where, respectively

$$y_1 = T^{-1/2} x_1 / L \quad ; \quad y_2 = T^{-1/2} \tag{16}$$

For convenience, the length ratio ξ is introduced, where

$$\xi = x_1 / L = y_1 / y_2 \tag{17}$$

The derivative R_ϕ should also vanish on windward and leeward meridians for lateral symmetry.

The appearance of cos ϕ in the only forcing function in Eq. (15), and the homogeneous boundary conditions along windward and leeward meridians, indicate that the solution has a similar variation with ϕ. Let

$$R(\phi, y) = R_0(y) + R_1(y) \cos \phi \tag{18}$$

Then, equating coefficients of cos ϕ and $(\cos \phi)^0$, one has an ordinary differential equation for $R_1(y)$

$$R_1'' - 2yR_1' + (R_1/y)' - (P - 1)R_1 = 2y\alpha/\tau \tag{19}$$

where primes indicate differentiation with respect to y; however, one has no information with regard to axisymmetric displacements R_0, such as might be caused by levels of internal pressures other than that for which the conic skirt was shaped.

An expression for the axisymmetric displacement R_0 can be developed by introducing a stress-strain relationship such as

$$(r - \tau x)_{sym}/\tau x = \left(T^\phi_{sym} - T^\phi_{ref}\right)/hE = 2\tau^3(P - P_{ref})qx/hE$$

where hE is thickness times the elastic modulus in hoop tension. In normalized variables

$$R_0 = C_R y^2 \quad , \quad C_R = \tau^2(P - P_{ref})(hE)^{-1}(2q_\tau x T^x)^{1/2}$$

Because R_0 here does not vanish at y_1 and y_2 as required in the present analysis, it appears that the ordering of magnitudes for the various terms in the differential equations (5) through (7) probably falls in a small neighborhood of the end constraint points. For example, the shear stress is expected to peak at the end points, and perhaps one of the shear terms is not negligible there when R_0 does not vanish identically.

We avoid this complication in the present analysis by limiting it to cases where R_0 is zero everywhere. As a result, the present analysis for $P > 1$ is apparently limited in validity to two cases: (1) the case in which the internal pressure is precisely that which produces a conic shape in elastic cloth at zero angle of attack ($P = P_{ref}$) and (2) the case in which the cloth is inelastic ($hE \to \infty$) so that the shape at zero angle of attack is conical for any level of pressurization provided $P > 1$.

Equation (19) does not seem to describe any of the common, tabulated mathematical functions. It can, of course, be integrated numerically to provide an R_τ/α profile for particular choices for $P - 1$, T, and ξ. Presented here are profiles for large and small values of the tension parameter T. Also presented, because of its critical importance in an application, is the variation of displacement slope at $x = L$ with T.

<u>$T \gg 1$</u>

In this high-altitude case, $y \ll 1$. We reduce Eq. (19) by neglecting the second and fourth left-member terms. The immediate solution is

$$R_1(y) = -(\alpha/\tau)(4y)^{-1}\left(y^2 - y_1^2\right)\left(y_2^2 - y^2\right) \qquad (20)$$

which is independent of pressurization level, $P > 1$. The maximum value of absolute displacement is given by

$$(r - \tau x)_{max} T/(\alpha L) = 6^{-3/2}[1 + \xi^2 + (1 + 14\xi^2 + \xi^4)^{1/2}]^{1/2} \times [-2(1 + \xi^2) + (1 + 14\xi^2 + \xi^4)^{1/2}] \tag{21}$$

which is plotted in the dashed line in Fig. 4. The maximum occurs at a value of $(y/y_2)^2$ that approaches 1/3 as $\xi \to 0$ (vanishing forecone) and that approaches $(1 + \xi^2)/2$ as $\xi \to 1^-$ (vanishing aftercone skirt).

$T \ll 1$

We reduce Eq. (19) by neglecting the third left-member term everywhere. The first left-member term contains the highest order derivative, R_1'', and is retained so that the reduced version of Eq. (19) has a solution that is uniformly valid in (y_1, y_2); i.e., it vanishes as required at both ends. Because $y \gg 1$, the solution can be further reduced to

$$R_1 = -2(\alpha/\tau)(P + 1)^{-1} y\left[1 - (y_1/y)^{(1+P)/2} - (1 - \xi^{(1+P)/2}) \times (y/y_2)^{(P-5)/2} \exp\left(y^2 - y_2^2\right)\right], \qquad y \gg 1 \tag{22}$$

In this low-axial-tension limit (low altitudes), the solution retains a dependence on pressurization level P. The solution in this limit has an interesting character. The displacement of the windward and leeward surfaces ($\pm R_1$) increases in magnitude linearly with distance from the forward attachment point until $1 - x/L$ is only $(T/2) \log (1/T)$. The displacement then vanishes abruptly as $x \to L$. The maximum value of the absolute displacement is approximately

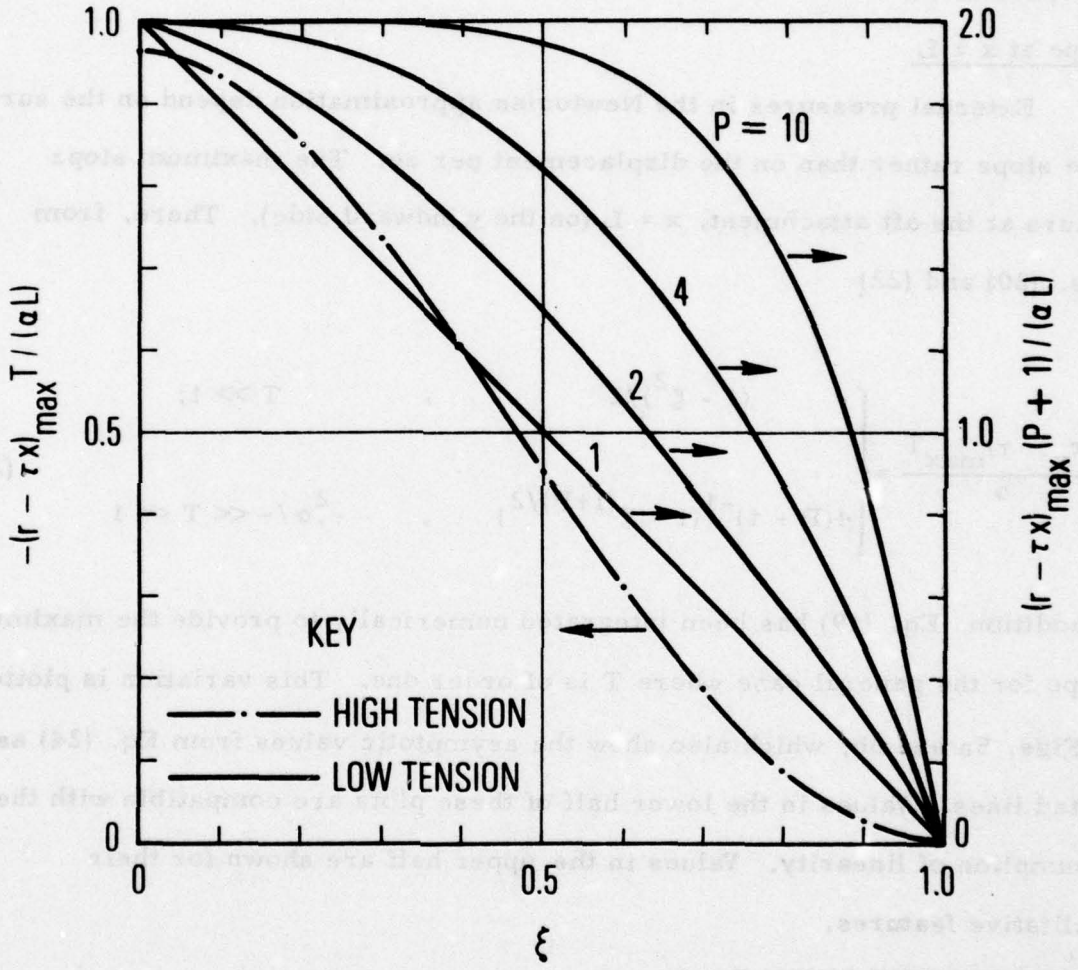

Fig. 4. Maximum Fabric Displacement in High- and Low-Tension Limits

$$(r - \tau x)_{max}/(\alpha L) = 2(P + 1)^{-1}(1 - \xi^{(1+P)/2}) \qquad (23)$$

This relation is plotted as the solid curves in Fig. 4 for four values of pressurization.

Slope at x = L

External pressures in the Newtonian approximation depend on the surface slope rather than on the displacement per se. The maximum slope occurs at the aft attachment, x = L (on the windward side). There, from Eqs. (20) and (22)

$$\frac{(r_x - \tau)_{max} T}{\alpha} = \begin{cases} (1 - \xi^2)/2 & , \quad T \gg 1; \\ 4(P + 1)^{-1}(1 - \xi^{(1+P)/2}) & , \quad \tau^2\alpha/\tau \ll T \ll 1 \end{cases} \qquad (24)$$

In addition, Eq. (19) has been integrated numerically to provide the maximum slope for the general case where T is of order one. This variation is plotted in Figs. 5a and 5b, which also show the asymptotic values from Eq. (24) as dotted lines. Values in the lower half of these plots are compatible with the assumption of linearity. Values in the upper half are shown for their qualitative features.

DISPLACEMENT WHEN P < 1

In terms of normalized variables R and y, Eq. (13) becomes

$$R_{yy} - 2yR_y + R_y/y - R/y^2 = y[1 - P + 2(\alpha/\tau)\cos\phi] \qquad (25)$$

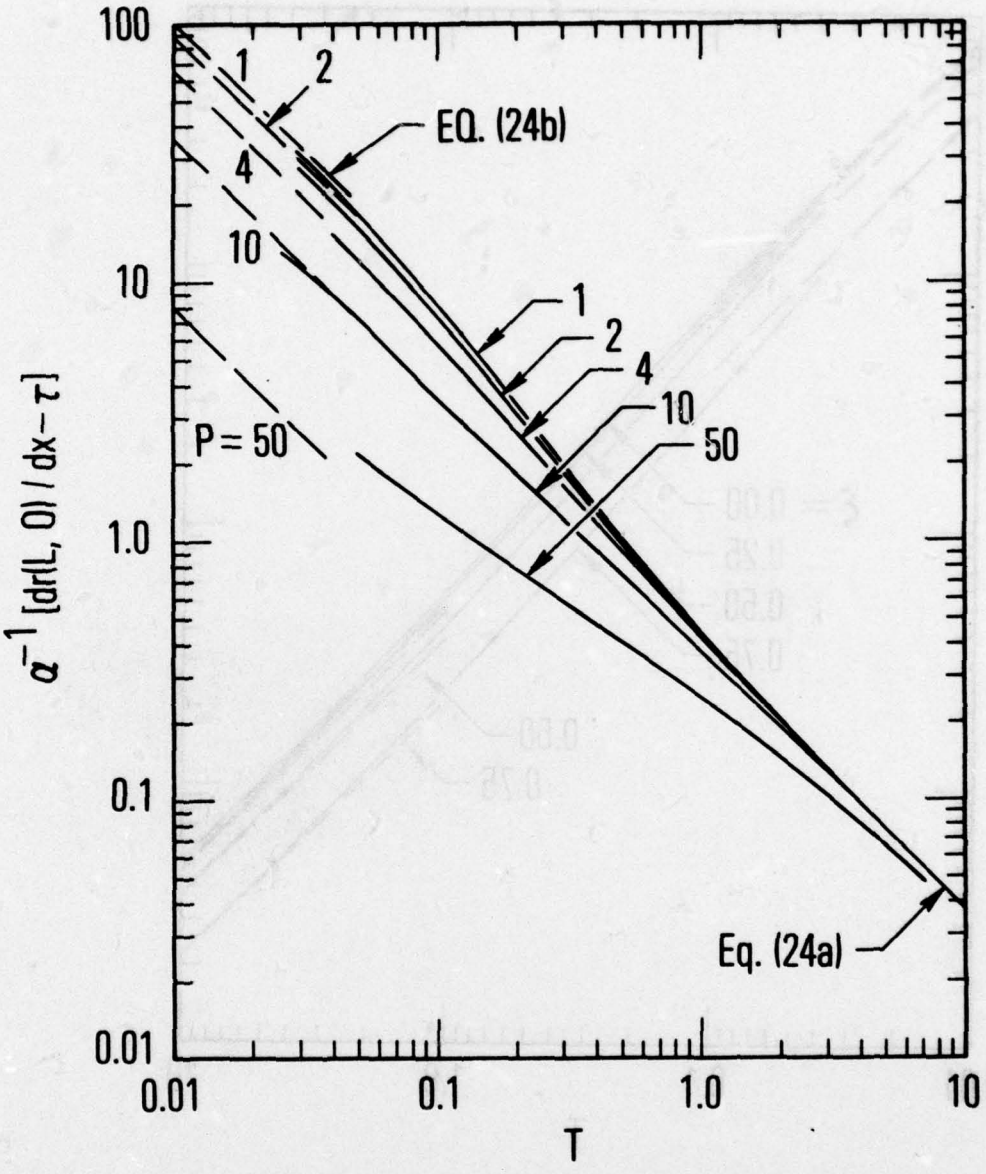

Fig. 5a. Surface Deflected Slope at x = L, ξ = 0.5

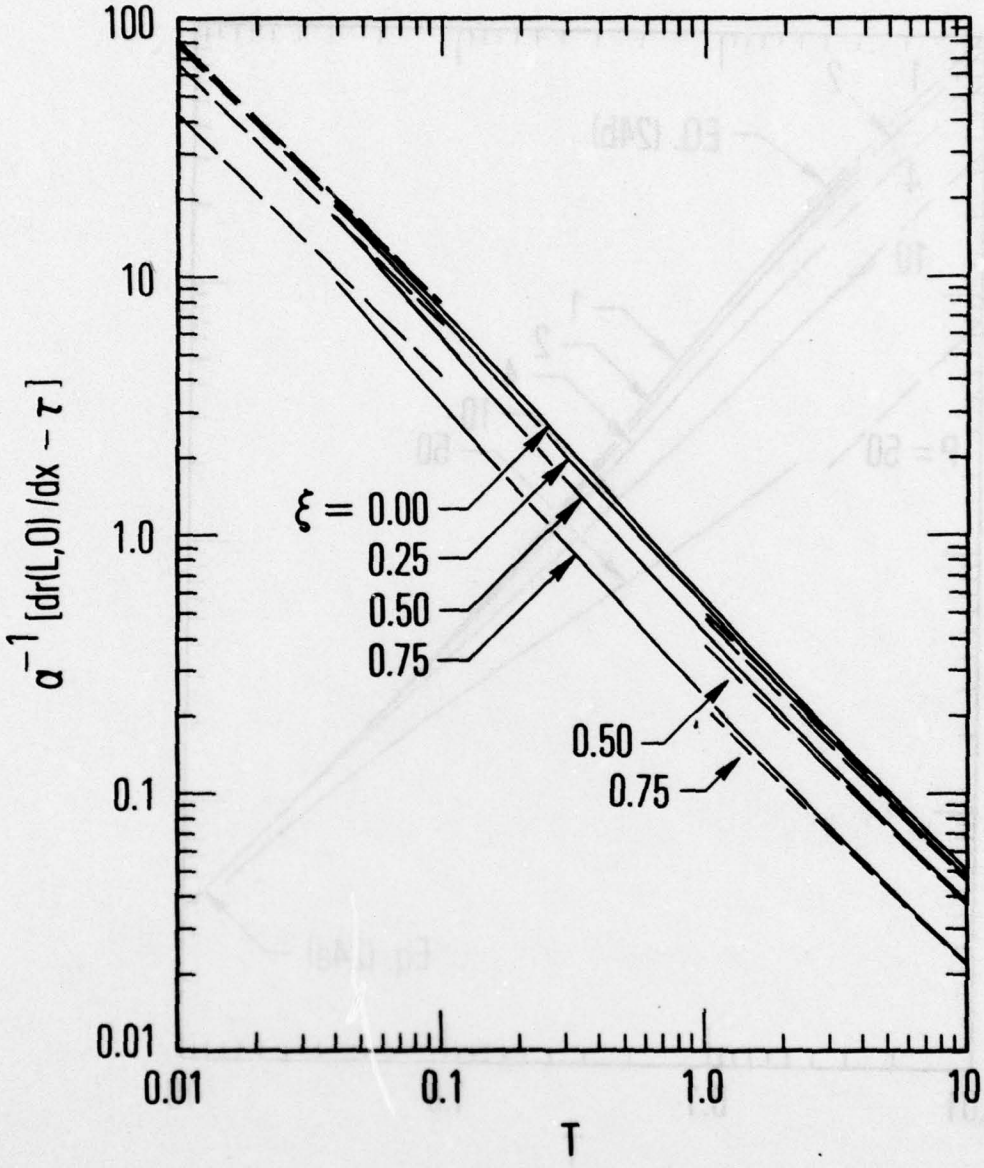

Fig. 5b. Surface Deflected Slope at x = L, P = 4

Again, a cosine variation of the form given in Eq. (18) is indicated. In the present instance, $R_1(y)$ is the same as for $P > 1$, and the symmetric part $R_o(y)$ is proportional

$$R_o(y) : (1 - P) :: R_1(y) : 2\alpha/\tau \tag{26}$$

Thus

$$R(\phi, y)_{P<1} = \frac{1 - P + 2(\alpha/\tau)\cos\phi}{2(\alpha/\tau)\cos\phi} R(\phi, y)_{P>1} \tag{27}$$

This eliminates the need for separate solutions for this case; the solution without folds in the skin ($P > 1$) is extended into the domain $0 < 1 - P \ll 1$, where the skin develops longitudinal folds (also called creases, fins, or strakes) but where the fractional reduction in circumference remains small.

FRUSTUM SECTION FORCES

For any level of internal pressure or displacement shape, the total axial and normal forces may be obtained by integrating external pressures. The external pressure coefficient can be expressed as

$$C_p/2\tau^2 = 1 + 2[R_y + (\alpha/\tau)\cos\phi] \tag{28}$$

The axial force per station X′, to first order in the small displacement scale, is

$$X'/q = 4\pi\tau^4 x(1 + 3R_o' + R_o/y) \tag{29}$$

and the normal force per station N′ is

$$N'/q = 4\pi\tau^3 x(R_1' + \alpha/\tau) \tag{30}$$

Equation (29) assures us that there is no change in axial force for $P > 1$, for then the symmetric displacement R_o vanishes in this essentially inelastic analysis. When $0 < 1 - P \ll 1$, this relation can be written

$$X'/q = 4\pi\tau^4 x\left[1 + \frac{1 - P}{2(\alpha/\tau)}(3R_1' + R_1/y)\right], \qquad P < 1 \tag{31}$$

BICONIC FORCE AND MOMENT COEFFICIENTS

The axial force coefficient C_x, based on base area in the present slender-body, Newtonian-pressure approximation is unchanged for $P > 1$; for $0 < 1 - P \ll 1$, however, C_x can be written as

$$C_x = 2\theta^2\xi^2 + (\pi\tau^2 L^2)^{-1}\int_{x_1}^{L}(X'/q)\,dx \tag{32}$$

which can be written, after an integration by parts, as

$$\frac{C_x - 2\tau^2 - 2(\theta^2 - \tau^2)\xi^2}{(1 - P)\tau^2} = -\frac{4T}{(\alpha/\tau)}\int_{y_1}^{y_2} R_1\,dy, \qquad P < 1 \tag{33}$$

The normal force coefficient slope, based on base area, can be expressed, by use of Eq. (30) and a similar integration by parts, as

$$C_{N_\alpha} - 2 = -\frac{4T}{(\alpha/\tau)}\int_{y_1}^{y_2} R_1\,dy, \qquad P \gtrsim 1 \tag{34}$$

Both Eqs. (33) and (34) have the same right member, and this is plotted in Figs. 6a and 6b for $\xi = 0.5$ and $P = 4$, respectively. Limiting values are

$$C_{N_\alpha} - 2 \sim \begin{cases} (4T)^{-1}(1 + 4\xi^2 \ln \xi - \xi^4), & T \gg 1; \\ 4(P+1)^{-1}(3-P)^{-1}[3 - P + (1+P)\xi^2 - 4\xi^{(1+P)/2}], & T \ll 1 \end{cases} \tag{35}$$

which are the dashed lines of Fig. 6.

The pitching moment coefficient slope, taken about the point $x = 0$ (theoretical nose) and based on base area and base diameter, is given by

$$\tau C_{M_\alpha} + 3^{-1}[2 + \xi^3(1 - \tau/\theta)] = 4T^{3/2}(\alpha/\tau)^{-1}\int_{y_1}^{y_2} yR_1\, dy \tag{36}$$

This static stability derivative is plotted in Figs. 7a and 7b for $\xi = 0.5$ and $P = 4$, respectively. Limiting values are

$$\tau C_{M_\alpha} + 3^{-1}[2 + \xi^3(1 - \tau/\theta)] \sim \begin{cases} -2(15T)^{-1}(1-\xi)^3(1 + 3\xi + \xi^2), & T \gg 1; \\ -(8/3)(P+1)^{-1}(5-P)^{-1} \\ \times[5 - P + (P+1)\xi^3 - 6\xi^{(1+P)/2}], & T \ll 1 \end{cases} \tag{37}$$

and these appear as dashed lines in Fig. 7.

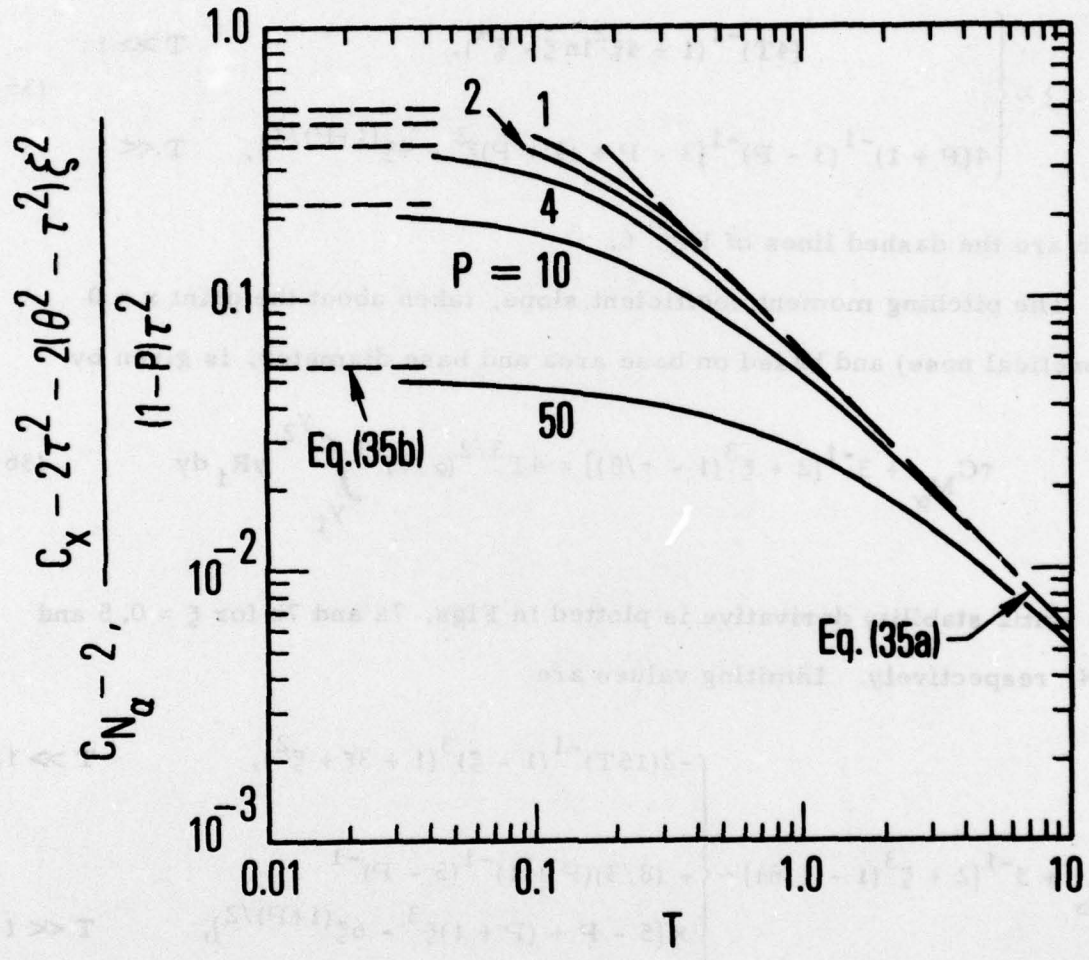

Fig. 6a. Axial and Normal Force Coefficient, $\xi = 0.5$

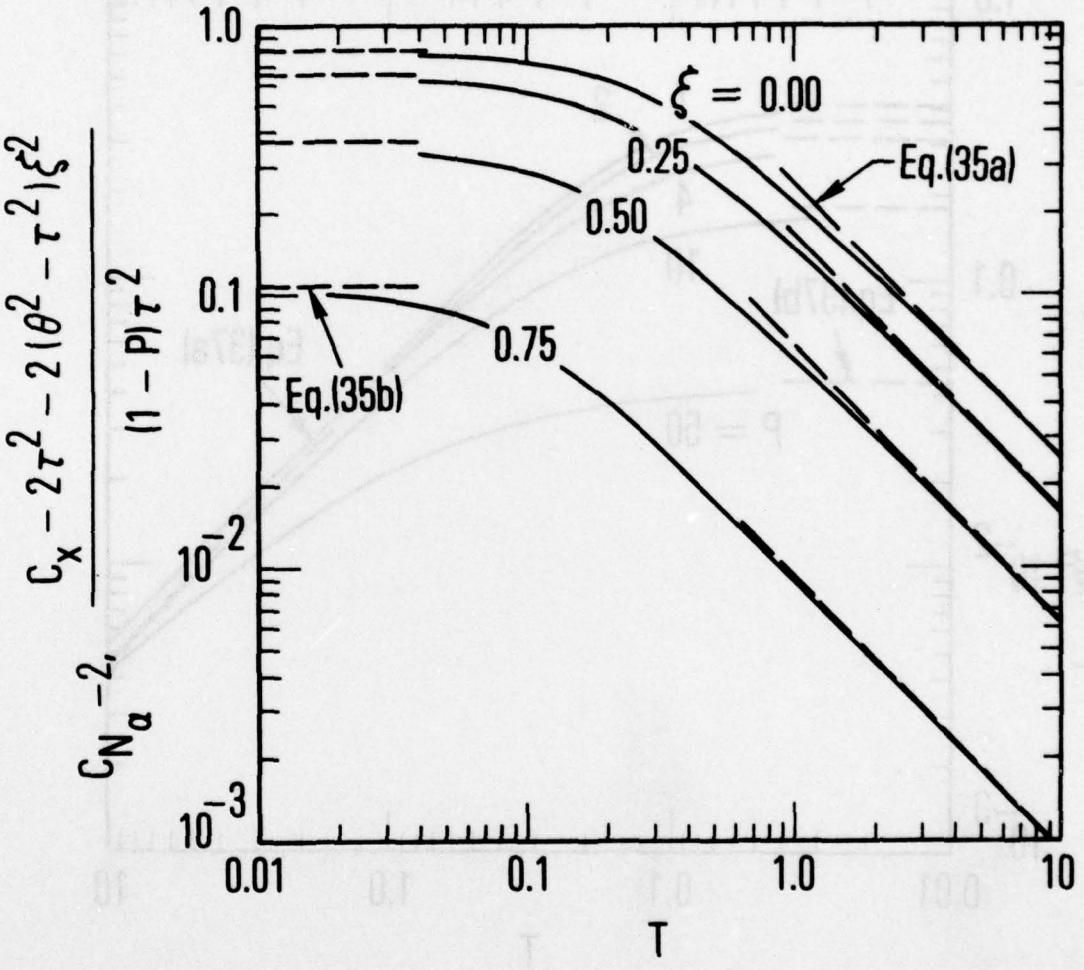

Fig. 6b. Axial and Normal Force Coefficient, P = 4

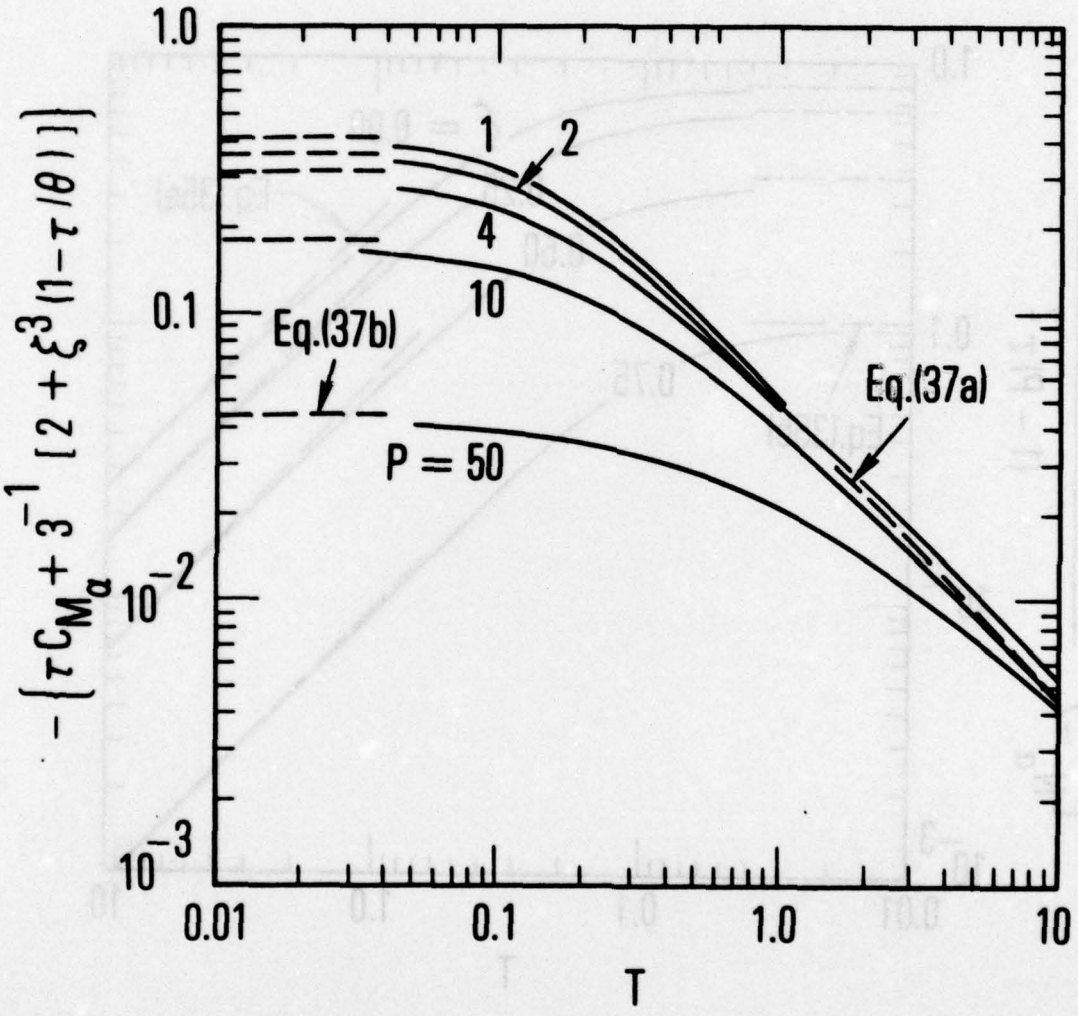

Fig. 7a. Pitching Moment Coefficient Slope, $\xi = 0.5$

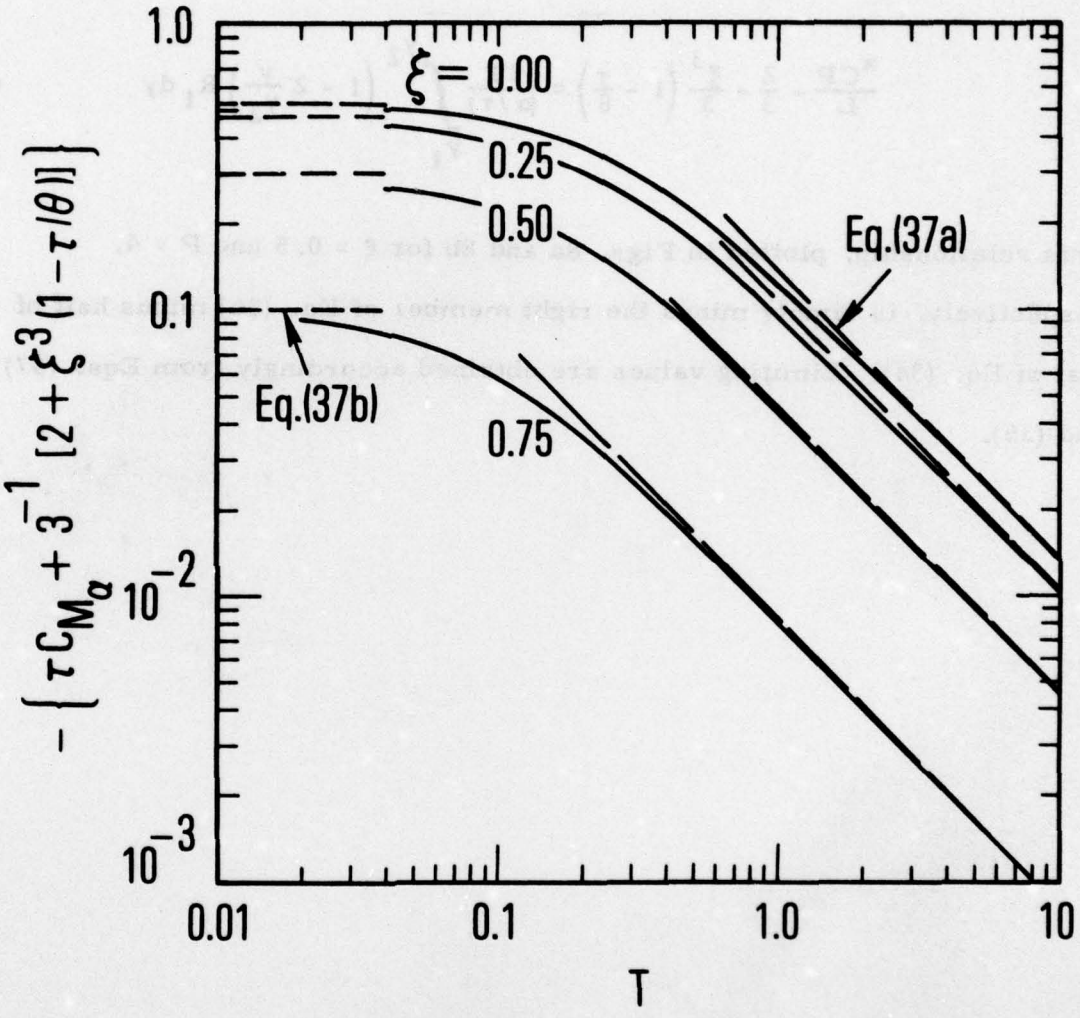

Fig. 7b. Pitching Moment Coefficient Slope, P = 4

The center-of-pressure location, expressed as a fraction of the theoretical length L, is given by

$$\frac{x_{CP}}{L} - \frac{2}{3} - \frac{\xi^3}{3}\left(1 - \frac{\tau}{\theta}\right) = \frac{2T}{(\alpha/\tau)} \int_{y_1}^{y_2} \left(1 - 2\,\frac{y}{y_2}\right) R_1\, dy \qquad (38)$$

This relationship, plotted in Figs. 8a and 8b for $\xi = 0.5$ and $P = 4$, respectively, is simply minus the right member of Eq. (36) minus half of that of Eq. (34). Limiting values are obtained accordingly from Eqs. (37) and (35).

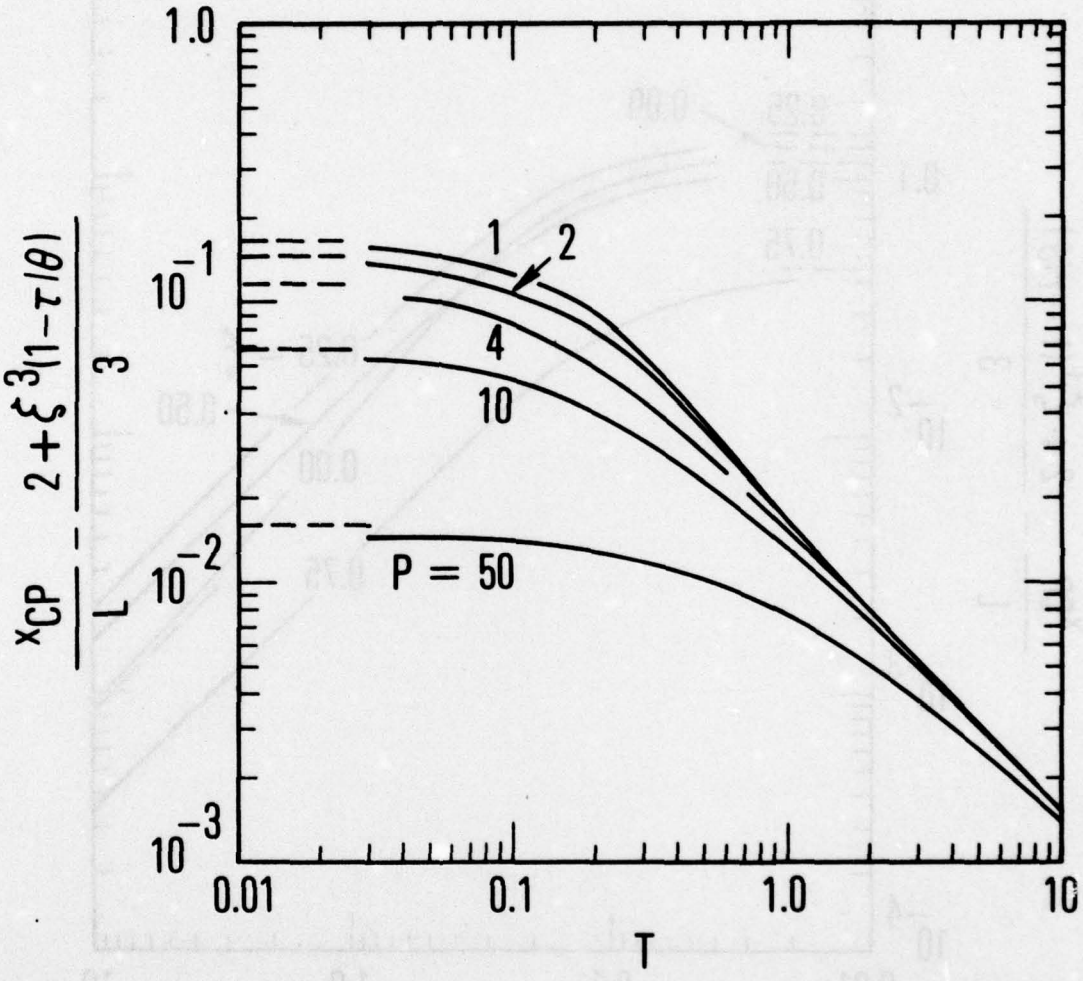

Fig. 8a. Center-of-Pressure Movement, $\xi = 0.5$

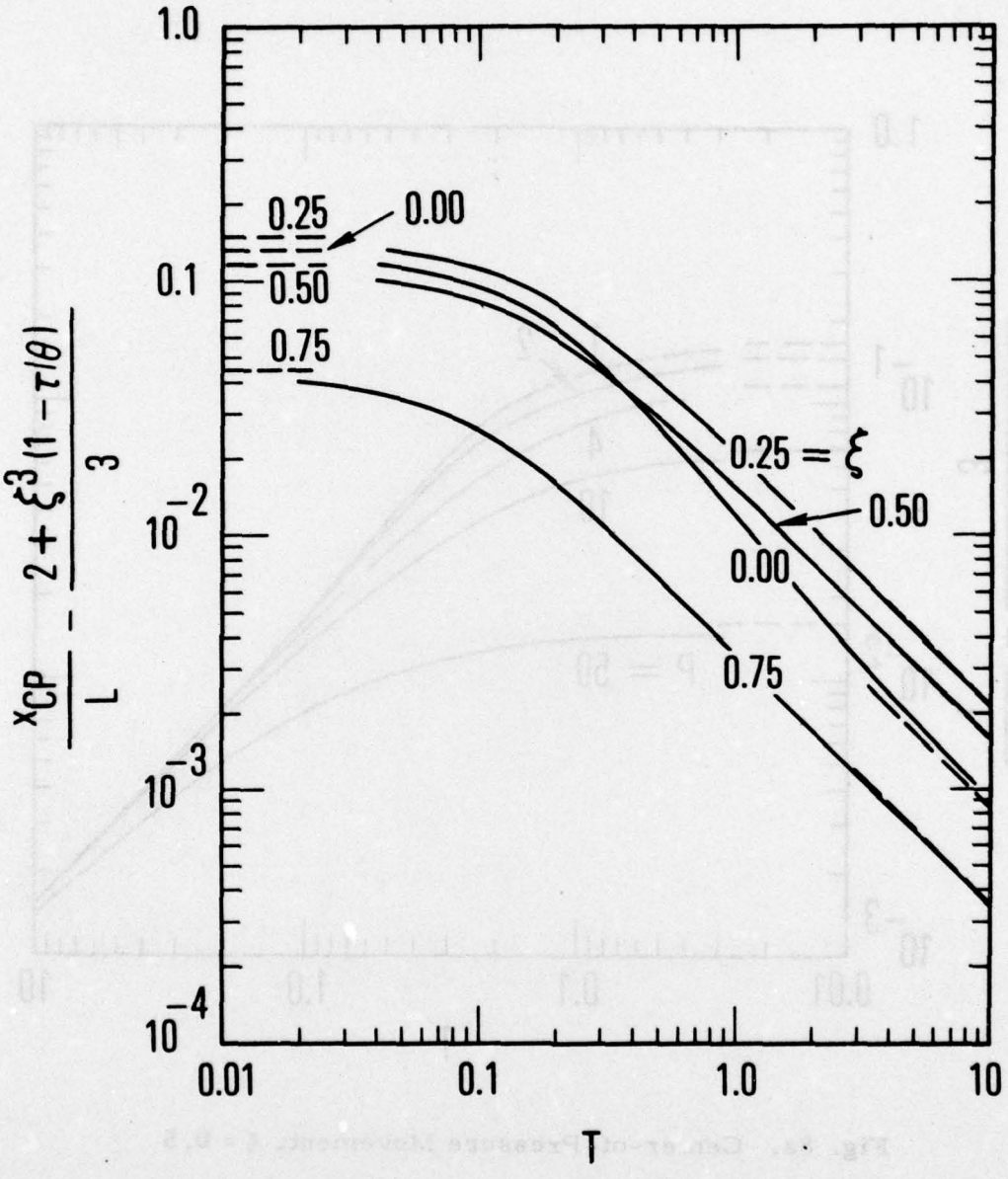

Fig. 8b. Center-of-Pressure Movement, P = 4

DISCUSSION

The present linearized theory has shown how "softening" the vehicle (increasing the dynamic pressure for given fabric tension) increases both static stability and static margin (Figs. 7 and 8). Also shown (Fig. 5) is how the slope of the fabric at the tail on the windward side increases dramatically as the tension parameter decreases. As this slope increases, so does local heating rate. Vehicle designs can be conceived where this effect is more critical than changes in the aerodynamic coefficients. Further, as the aft fabric slope increases, local external pressure may climb above the given internal pressure level. Such pressures would surely create folds (strakes) in the fabric, with radical aerodynamic and dynamic consequences.

From these considerations, it is concluded that inflated membrane biconics are useful only in environments where the tension parameter T, defined in Eq. (9), is at least of order one. Further, it appears that this useful range of T cannot be appreciably extended by increasing the pressurization level P, where P is $p_i/2\ \tau^2 q$), unless P is at least an order of magnitude greater than one.

THE IVAN A. GETTING LABORATORIES

The Laboratory Operations of The Aerospace Corporation is conducting experimental and theoretical investigations necessary for the evaluation and application of scientific advances to new military concepts and systems. Versatility and flexibility have been developed to a high degree by the laboratory personnel in dealing with the many problems encountered in the nation's rapidly developing space and missile systems. Expertise in the latest scientific developments is vital to the accomplishment of tasks related to these problems. The laboratories that contribute to this research are:

Aerophysics Laboratory: Launch and reentry aerodynamics, heat transfer, reentry physics, chemical kinetics, structural mechanics, flight dynamics, atmospheric pollution, and high-power gas lasers.

Chemistry and Physics Laboratory: Atmospheric reactions and atmospheric optics, chemical reactions in polluted atmospheres, chemical reactions of excited species in rocket plumes, chemical thermodynamics, plasma and laser-induced reactions, laser chemistry, propulsion chemistry, space vacuum and radiation effects on materials, lubrication and surface phenomena, photosensitive materials and sensors, high precision laser ranging, and the application of physics and chemistry to problems of law enforcement and biomedicine.

Electronics Research Laboratory: Electromagnetic theory, devices, and propagation phenomena, including plasma electromagnetics; quantum electronics, lasers, and electro-optics; communication sciences, applied electronics, semiconducting, superconducting, and crystal device physics, optical and acoustical imaging; atmospheric pollution; millimeter wave and far-infrared technology.

Materials Sciences Laboratory: Development of new materials; metal matrix composites and new forms of carbon; test and evaluation of graphite and ceramics in reentry; spacecraft materials and electronic components in nuclear weapons environment; application of fracture mechanics to stress corrosion and fatigue-induced fractures in structural metals.

Space Sciences Laboratory: Atmospheric and ionospheric physics, radiation from the atmosphere, density and composition of the atmosphere, aurorae and airglow; magnetospheric physics, cosmic rays, generation and propagation of plasma waves in the magnetosphere; solar physics, studies of solar magnetic fields; space astronomy, x-ray astronomy; the effects of nuclear explosions, magnetic storms, and solar activity on the earth's atmosphere, ionosphere, and magnetosphere; the effects of optical, electromagnetic, and particulate radiations in space on space systems.

THE AEROSPACE CORPORATION
El Segundo, California